Precritical anomalous scaling and magnetization temperature dependence in cubic ferromagnetic crystals

Igor Kolokolov [1,2,*] Victor S. L'vov [3,†] and Anna Pomyalov [4,‡]

[1] *L. D. Landau Institute for Theoretical Physics, Ak. Semenova 1-A, Chernogolovka 142432, Moscow region, Russia*

[2] *National Research University Higher School of Economics, 101000, Myasnitskaya 20, Moscow, Russia*

[3] *Department of Physics of Complex Systems, Weizmann Institute of Science, Rehovot 76100, Israel*

[4] *Department of Chemical and Biological Physics, Weizmann Institute of Science, Rehovot 76100, Israel*

(Received 13 December 2024; revised 15 March 2025; accepted 18 March 2025; published 26 March 2025)

Recent developments in spintronics have drawn renewed attention to the spin dynamics of cubic ferromagnetic crystals EuO and EuS. These ferromagnets have the simplest possible magnetic structure, making them the most suitable systems for testing various theoretical models of magnetic materials. A commonly used Weiss mean-field approximation (MFA) provides only a qualitative description of the magnetization temperature dependence $M(T)$. We develop a consistent theory for $M(T)$ based on the perturbation diagrammatic technique for spin operators. Our theory is in excellent quantitative agreement with the experimental dependence of $M(T)$ for EuO and EuS throughout the entire temperature range from $T = 0$ to Curie temperature T_C. In particular, our theoretical dependence $M(T)$ demonstrates a scaling behavior $M(T) \propto (T_C - T)^{\beta_*}$ with the scaling index $\beta_* \approx 1/3$ in a wide range of temperatures, in agreement with the experimentally observed apparent scaling in EuO and EuS. The scaling behavior with $\beta_* \approx 1/3$ is manifested in the temperature range $T \lesssim T_C$ where corrections to the magnetization due to its fluctuations $\delta M(T) \lesssim M(T)$. To distinguish it from the narrow "critical" range $T \approx T_C$ with $\delta M(T) > M(T)$, we term this T-range "precritical." The precritical corrections $\delta M(T)$ are still large enough to affect the $M(T)$ behavior. The index β_* fundamentally differs from the "normal" scaling index $\beta_{MFA} = 1/2$ predicted by the MFA, which neglects the magnetization fluctuations. We refer to the apparent magnetization scaling with $\beta_* \approx 1/3$, which emerges in our theory, as "precritical anomalous."

DOI: 10.1103/PhysRevB.111.104433

I. INTRODUCTION

A. Ferromagnetic EuO and EuS

The development of spintronics has generated significant interest in rare-earth oxide ferromagnetic semiconductors, such as europium chalcogenides EuO and EuS. In particular, EuO is especially promising for applications [1] as it has the third strongest saturation magnetization of all known ferromagnets [2], one of the largest magneto-optic Kerr effects [3], a pronounced insulator-to-metal transition [4–6], as well as a colossal magnetoresistance effect [7].

Moreover, among various magnetically ordered materials, EuO and EuS are probably the most suitable systems for testing various theoretical models of magnetic material because they are well-studied experimentally and have a simple crystallographic structure. Unlike other well-known magnetics, such as yttrium iron garnet (YIG), which has 80 atoms in the unit cell, with 20 of them (Fe) possessing a magnetic moment [8], EuO and EuS are the only known ferromagnets having two atoms in the unit cell, with only one of them (Eu^{+2}, with spin $S = 7/2$) having a magnetic moment. The crystallographic structure of EuO and EuS [face-centered-cubic (fcc) lattice] is illustrated in Fig. 1.

B. Plan of the paper and main results

This paper aims to describe and improve a theory of spontaneous magnetization $M(T)$ of ferromagnetics over an entire temperature range from $T = 0$ to Curie temperature T_C, at which $M = 0$. The theory is evaluated by comparing it with the existing experimental data [9–11]. Instead of using the normalized magnetization $M(T)/M(0)$, which is assumed to be aligned with the small external magnetic field $\boldsymbol{h} = \{0,\ 0,\ h_z\}$, we adopt a more convenient approach from the theoretical viewpoint to use the normalized $\hat{\boldsymbol{z}}$-projection of the mean spin $\overline{S}_z(T)/S = M(T)/M(0)$. The mean spin $\overline{S}_z$ is defined as

$$\overline{S}_z = \frac{1}{N_{\rm lat}} \left\langle \sum_j S_j^z \right\rangle. \tag{1}$$

Here S_j^z is the local spin projection on the external magnetic field, j runs over magnetic ion lattice sites per unit volume, and $N_{\rm lat}$ is their number.

In Fig. 2(a), we plot the experimental results for the normalized mean spin $\overline{S}_z(T)/S$ for EuO (main panel, a solid black line with circles) and EuS (inset, a solid blue line with squares). The experimental Curie temperatures $T_C^{\rm exp} = 69.2$ K for EuO and $T_C^{\rm exp} = 16.6$ K for EuS are clearly visible in the figure. Note that the properties of EuO and EuS are sensitive to stoichiometry and the presence of defects (see, for example, [13,14]). In this work, we do not address these technological

*Contact author: kolokol@itp.ac.ru

†Contact author: victor.lvov@gmail.com

‡Contact author: anna.pomyalov@weizmann.ac.il

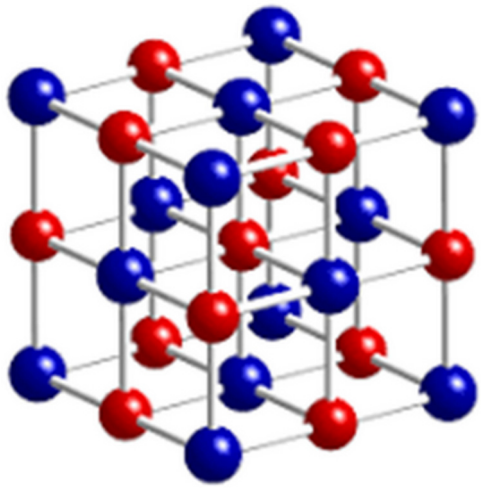

FIG. 1. fcc crystallographic structure of EuO and EuS. Blue balls represent Eu atoms, and red balls represent oxygen (O) or sulfur (S) atoms. The lattice constant is $a = 5.14$ Å for EuO and $a = 5.96$ Å for EuS. Curie temperatures are $T_C = 69.2$ K for EuO and $T_C = 16.6$ K for EuS. In both structures, the coordination number of the Eu atoms is $Z = 12$. For additional parameters, see Table I.

issues, and we refer to the experiments in which the material properties are well controlled.

The experimental dependencies of $\overline{S}_z/S$ on the normalized temperature $T/T_C^{\rm exp}$ for both materials practically coincide, as is observed in Fig. 2(b). This allows us to focus on the theory-experiment comparison mainly for one material. For concreteness, we choose EuO. The relevant parameters of EuO and EuS are listed in Table I.

The rest of the paper is organized as follows.

Section II is devoted to the historical and physical background of the problem. In Sec. II A, we provide a brief overview of the achievements and fundamental problems of the celebrated classical Weiss mean-field approximation (MFA) [15], and we recall in Sec. II B their resolution by Heisenberg, who introduced the exchange interaction of quantum-mechanical origin into the original Weiss MFA [16].

The quantum version of the Weiss-Heisenberg (WH) MFA, as represented by (10), provides a simple yet reasonable description of the temperature dependence of magnetization (or the mean value of the spin projection on the external magnetic field $\overline{S}_z$). A numerical solution of Eq. (10) for EuO, plotted in the main panel of Fig. 2(a) by a dotted blue line labeled (1), gives the WH-MFA value of the Curie temperature (where $\overline{S}_z = 0$), $T_C^{\rm WH} \approx 86.6$ K for EuO (about 20% larger than its experimental value $T_C^{\rm exp} \approx 69.2$ K).

The numerical solution for EuS, shown in the inset in Fig. 2(a), yields $T_C^{\rm WH} \approx 21.4$ K (to be compared with $T_C^{\rm exp} \approx 16.6$ K).

However, some problems with the WH-MFA still remain. For example, in the low-temperature limit, when $S - \overline{S}_z \ll S$, Eq. (10) predicts exponential decay of $\overline{S}_z$ with T, while a well-established spin-wave theory gives $S - \overline{S}_z \propto T^{3/2}$; see, for example, Ref. [17].

Vaks, Larkin, and Pikin solved this problem [18,19] using a developed diagrammatic technique (DT) for ferromagnetics in thermodynamic equilibrium, as briefly outlined in Appendix 1. However, their approach resulted in an unphysical behavior of $\overline{S}_z(T)$ near T_C, where the calculated corrections to $\overline{S}_z$ become infinite.

To resolve this issue and obtain a regularized description of $\overline{S}_z(T)$ across the entire range of T from $T = 0$ to $T = T_C$, we develop in Appendix the DT for spin operators, based on the functional representation of the generating functional $\mathcal{Z}(\boldsymbol{h})$, introduced and analyzed in Appendix 3. The first-order correction in the inverse coordination number $1/Z$ to the WH-MFA, $\delta\overline{S}_z(T) \simeq S/Z$, may be found in the one-loop approximation for the effective potential formulated in Appendix 4. The resulting Eq. (12) is presented in Sec. III A. The numerical solution of these equations for EuO is shown in Fig. 2(a) by the solid blue line labeled (2). It decays much faster than the blue dotted line for the WH-MFA with its exponential decay from the value S (not discernible for $T \lesssim 15$ K). More detailed analysis [not shown in Fig. 2(a)] indicates that the difference $S - \overline{S}_z$ is proportional to $T^{3/2}$, as expected from the low-temperature suppression of $\overline{S}_z$ by spin waves; see, e.g., Ref. [17].

In addition, we observe that the numerical solution of Eq. (12) is in good quantitative agreement with the experiment conducted in EuO (solid black line with circles) up to about 65 K. At this temperature, $\overline{S}_z(T)$ decreases twice, reaching $S/2$.

However, for larger T ($T \gtrsim 65$ K in EuO), Eqs. (12) give a slower decrease of $\overline{S}_z(T)$ than in the experiment, with the same $T_C^{\rm WH}$ (≈86.6 K for EuO) as in the WH-MFA. The reason for this inconsistency is explained in Sec. III B, which provides a brief overview of the Belinicher-L'vov (BL) DT [20]. Equations (12) with $1/Z$ corrections do not adequately consider the impact of the spin wave on the average spin projection $\overline{S}_z(T)$ for temperatures close to T_C (specifically, between $0.8T_C$ and T_C). The key advantage of the BL DT is that it takes into account, order-by-order, the kinematic relationship (22) between the spin correlations, which relates transverse spin correlators describing propagating spin waves and longitudinal correlators [including $\overline{S}_z(T)$]. As shown in Sec. III C, this allows us to account for the effect of spin waves even in the zero-order approximation, i.e., in the MFA.

The numerical solution of the resulting spin-wave-improved WH-MFA (23), shown in Fig. 2(a) for EuO by a dashed green line labeled (3), demonstrates much better

TABLE I. Important parameters of EuO and EuS: the magnetization at zero temperature M_0; nearest neighbors J_1 and next-nearest neighbors J_2 exchange integrals; the experimental value $T_C^{\rm exp}$ of the Curie temperature; the "theoretical" $T_C^{\rm th}$ Curie temperature in the quantum Weiss-Heisenberg MFA, (11a); Curie temperature $\widetilde{T}_C^{\rm th}$, Eq. (26c) in the spin-improved MFA. Experimental [10] $\beta_{\rm exp}$ and theoretical β_* values of the apparent scaling index β that governs the temperature dependence of the magnetization $M(T) \propto (T_C - T)^\beta$ below T_C.

	M_0 Oe	J_1, K	J_2 K	$T_C^{\rm exp}$ K	$T_C^{\rm th}$ K	$\widetilde{T}_C^{\rm th}$ K	$\beta_{\rm exp}$	β_*
EuO	1920	1.25	0.25	69.2	86.6	66.5	0.36 ± 0.01	0.34 ± 0.02
EuS	1115	0.44	-0.2	16.6	21.4	13.7	0.36 ± 0.01	0.34 ± 0.02

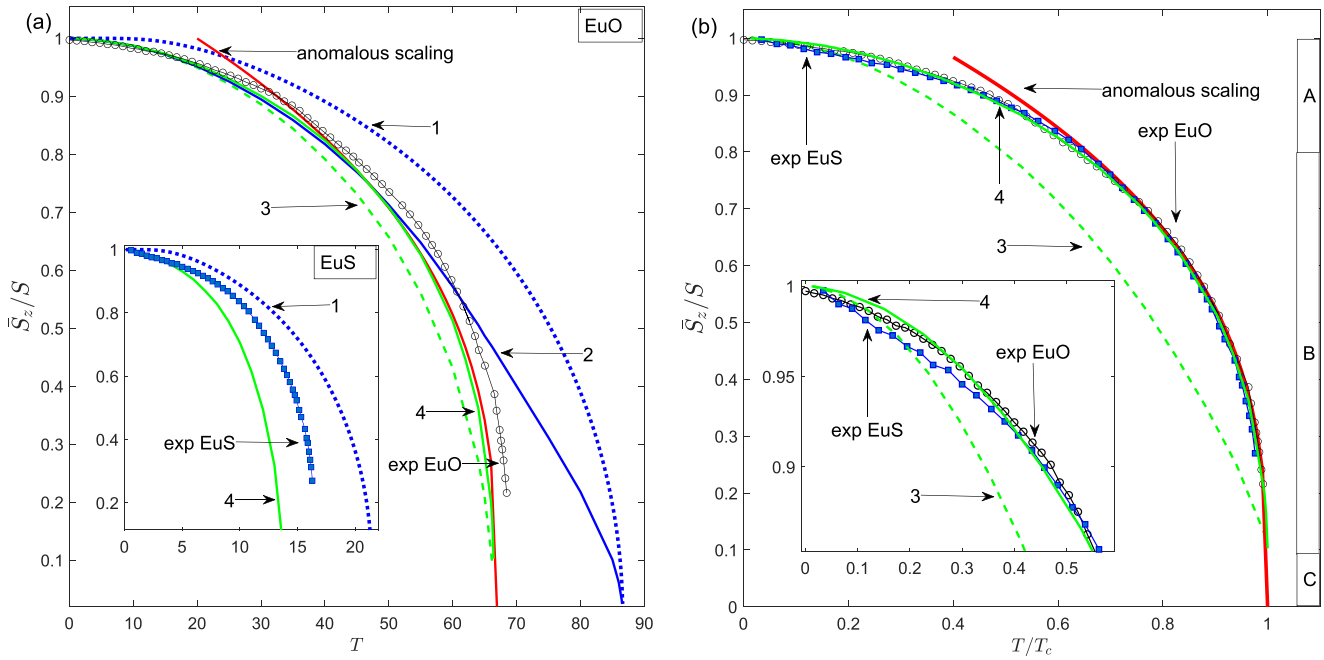

FIG. 2. Experimental and numerical results for $\overline{S}_z/S$ vs T [panel (a)] and vs $T/T_{\rm c}$ [panel (b)]. In panel (a), the results for EuO are summarized in the main panel, and those for EuS are summarized in the inset. The inset in (b) gives a closeup of the low-T range for the same data as in the main panel of (b). Experimental results [9–11] for EuO are plotted as solid black lines with circles, and those for EuS are plotted by solid blue lines with squares. The results of numerical solutions are denoted as follows: (1) Quantum version (10) of the Weiss-Heisenberg MFA for EuO in the main panel and for EuS in the inset of (a)—dotted blue lines. (2) $1/Z$-corrected equation of the Weiss-Heisenberg MFA (12) for EuO—solid blue line. Recall that $Z = 12$ is the coordination number of Eu atoms; see Fig. 1. (3) Spin-wave-improved version of the MFA (23) for EuO—dashed green line. (4) Spin-wave-improved version with the first-order $1/Z$ corrections (27) for EuO in the main panel of (a) and (b), and for EuS in the inset of (a)—solid green line. The red line represents the power-law fit to the solution of Eq. (27) in the form $a_{\rm th}(T_{\rm c} - T)^{\beta_*}$, $\beta_* = 0.34 \pm 0.02$ with $T_{\rm c} = 66.5$. The predicted coefficients are $a_{\rm th} = 0.27$ in (a) and $a_{\rm th} = 1.15$ in (b). Three regimes of $\overline{S}_z(T)/S$ behavior dominated by various types of magnetization fluctuations are marked in (b). In the low-temperature "spin-wave-dominated" regime A, the T-dependence of $\overline{S}_z(T)$ is determined by the excitation level of spin waves (the transversal fluctuations of spins). In the precritical regime B, moderate transversal and longitudinal fluctuations are equally important, leading to deviation from MFA predictions. In the critical regime C, the corrections to the mean spin exceed its mean value, and the MFA, along with all our corrections, is no longer valid. Other approaches (e.g., the renormalization-group approach [12]) are required in this regime.

agreement with the experiment than all previous approaches. In particular, it includes low-temperature spin-wave corrections, proportional to $T^{3/2}$, and it coincides in this respect with the $1/Z$-corrected MFA (12). In addition, it decreases much faster than the solution of Eqs. (12), with T increasing toward $T = T_{\rm c}$, in agreement with the experimental behavior of $\overline{S}_z(T)$. As a result, it reaches zero at $\widetilde{T}_{\rm c}^{\rm th}$ (66.5 K for EuO), which is essentially closer to $T_{\rm c}^{\rm exp}$ (69.2 K for EuO) than the previous result (86.6 K for EuO). The spin waves are highly excited in the vicinity of $T = T_{\rm c}$, suppressing $\overline{S}_z(T)$ according to the kinematic relationship (22). Therefore, the mean-field value [proportional to $\overline{S}_z(T)$] is smaller, and consequently, the value of $T_{\rm c}$ decreases.

Further improvement of our results for $\overline{S}_z(T)$ is given in Sec. III C 3, where we present the $1/Z$-corrected spin-wave-improved MFA, summarized in Eq. (27). The numerical solutions of these equations are shown by a solid green line labeled (4) in the main panel of Fig. 2(a) for EuO and in the inset for EuS. The calculated Curie temperatures remain identical to those in the uncorrected spin-wave-improved scenarios, as follows from Eq. (21). However, $1/Z$ corrections significantly improve the behavior of $\overline{S}_z(T)$ at intermediate temperatures, bringing it much closer to experimental results. This improvement for EuO is evident in Fig. 2(a) by comparing the dashed (3) and solid (4) green lines.

Small discrepancies between the calculated and observed Curie temperatures may stem from the approximate nature of the theory, uncertainty of the exchange integrals, or limited accuracy of the Curie temperature measurements. Leaving these differences aside, we plotted in Fig. 2(b) the temperature dependences of $\overline{S}_z(T)$ versus normalized temperature $T/T_{\rm c}$, using $T_{\rm c} = T_{\rm c}^{\rm exp}$ for the experimental curves and their own values of $T_{\rm c}$ for the numerical curves. We observe excellent quantitative agreement between the theoretical dependence $\overline{S}_z(T/T_{\rm c})$, shown by the solid green line, and the experimental results, represented by the solid black line with circles for EuO, and the blue line with squares for EuS. All three lines coincide in the entire range of temperatures from $T = 0$ to $T \approx T_{\rm c}$.

It is important to emphasize that the power-law scaling of the magnetization is commonly measured in the reduced temperature range $(1 - T/T_{\rm c}) \lesssim 0.1$ corresponding to about half of the reduced magnetization range $M/M(0) \lesssim 0.5$. This definition does not reflect the physical origins of $M(T)$ behavior. We distinguish between the intermediate precritical range of temperatures $0.7\,T_{\rm c} \lesssim T < T_{\rm c}$, where $\overline{S}_z/S$ decreases

from about 0.7 to about 0.1, and the critical range with $\overline{S}_z/S \lesssim 1/Z \approx 0.1$. In the precritical range, the experimental and theoretical curves of $\overline{S}_z(T)$ closely follow the power-law-like behavior $\overline{S}_z(T) \propto (T_c - T)^{\beta_*}$ (plotted in Fig. 2 as a solid red line). The apparent precritical anomalous scaling index is estimated to be $\beta_* \approx 0.34 \pm 0.01$, which is in good agreement with the experimental value $\beta_{\rm exp} = 0.36 \pm 0.015$ reported in [10]. Moreover, it agrees well with the critical scaling index $\beta_{\rm cr} \approx 0.365$ derived from the renormalization-group theory for the 3D Heisenberg model [12].

We summarize our results in Sec. IV.

II. HISTORICAL AND PHYSICAL BACKGROUND

A. Classical Weiss mean-field approximation

The theoretical description of ferromagnetism has a long history, starting with the celebrated Weiss's mean-field approximation first published in 1907 [15]. Shortly before this, Langevin developed his theory of paramagnetism, based on the fundamental idea that the orientation of a molecular dipole of moment μ in a field H is governed by the Boltzmann distribution law. If so, the magnetic momentum per unit volume [the magnetization $M(T)$] is given by the expression

$$M = M_0 L\left(\frac{\mu H}{T}\right), \quad M_0 = N_{\rm lat}\mu, \quad L(x) = \coth x - \frac{1}{x}, \tag{2}$$

where M_0 is the magnetization at $T \to 0$, $L(x)$ is the Langevin function [21], $\mu = S\mu_{\rm B}$, S is the spin of the magnetic ion, and $\mu_{\rm B} = \hbar e/2mc$ is the Bohr magneton, where $\hbar$ is the reduced Planck constant, e and m are the electron charge and mass, and c is the speed of light.

The basic idea of the Weiss MFA is that the effective field acting on an elementary magnet in a ferromagnetic medium is not the applied field H, but rather $H + gM(T)$, where $M(T)$ is the magnetization at a given temperature, and g is some temperature-independent factor. The term $gM(T)$ is called the "self-consistent molecular field" and is clearly a manifestation of some cooperative phenomenon.

With this modification, Eq. (2) becomes

$$M = M_0 L[\mu(H + gM)/T]. \tag{3a}$$

For small T, Eq. (3a) describes magnetization saturation at the level M_0. For very large T, the argument x of the Langevin function becomes small, and $L(x)$ can be approximated as

$$L(x) = \frac{x}{3} - \frac{x^3}{45} + \cdots \quad \text{for } x \ll 1. \tag{3b}$$

Accounting only for the first term in expansion (3b), we reduce Eq. (3a) to

$$\chi = M/H \approx \frac{M_0\mu}{[3(T - T_c)]}, \quad T_c = g\mu M_0/3. \tag{3c}$$

Here χ denotes the susceptibility M/H, which formally diverges at some critical temperature T_c known as the "Curie-Weiss temperature."

For $H = 0$ and T slightly below T_c, Eqs. (3a) and (3b) give

$$M(T) = M_0\sqrt{\left(1 + \frac{2T^2}{3T_c}\right)\left(1 - \frac{T}{T_c}\right)}. \tag{4a}$$

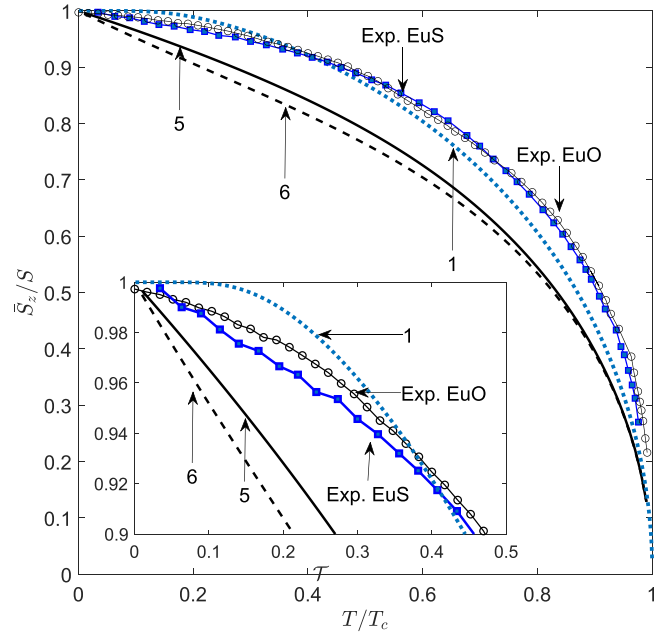

FIG. 3. Comparison between magnetization temperature dependencies $\overline{S}_z/S$ vs normalized temperature T/T_c obtained from (1) numerical solution of the WH-MFA (10)—blue dotted line, the same as line (1) in Fig. 2; (5) classical Weiss MFA, numerical solution of Eq. (4b)—solid black line; (6) interpolation formula (4a)—dashed black line. Experiments in EuO (solid black line with circles) and EuS (solid blue line with squares) are shown by the same line types as in Fig. 2.

The interpolation formula (4a), plotted in Fig. 3 as a dashed black line labeled (6), is exact in the limit $T \to T_c$ and normalized such that $\overline{S}_z(0) = S$. It is very close to the numerical solution of Eq. (3a) for $H = 0$, which takes the form

$$M(T) = M_0 L\left[\frac{3M}{M_0}\left(\frac{T}{T_c}\right)^{2/3}\right]; \tag{4b}$$

see the solid black line labeled (5) in Fig. 3.

Undoubtedly, Eqs. (3) and (4) represent the most significant result of Weiss's theory. They predict the critical temperature T_c. As this temperature is reached from below, $M(T)$ gradually decreases to zero. Beyond this temperature, $M(T)$ vanishes, consistent with observations from numerous experiments.

However, in 1907, when Weiss published his paper [15], there was a problem with the obtained values of T_c, Eq. (3c). At that time, the only known interaction between magnetic moments was the classical dipole-dipole interaction, leading to the so-called demagnetization magnetic field, which depends on the shape of the sample. For example, for the orthogonally magnetized film, $g = 4\pi$, and for the spherical sample, $g = 4\pi/3$. Taking for concreteness $g = 4\pi/3$, and actual EuO values $M_0 \approx 1920$ Oe and $\mu = 7\mu_{\rm B}$, Eq. (3c) gives $T_c \approx 3.77$ K, which is far below its experimental value $T_c^{\rm exp} \approx 70$ K.

The situation is even worse for yttrium iron garnet (YIG), the ferrimagnetic widely used in fundamental studies [8] and applications [22]. With $M_0 \approx 155$ Oe, $\mu = 5\mu_{\rm B}$, $g = 4\pi/3$ (for the sphere), Eq. (3c) gives $T_c \approx 0.22$ K, which has

nothing in common with the experimental value $T_c^{exp} \approx 560$ K. However, Weiss was courageous enough to publish his article despite the significant discrepancy between the predicted and experimental values of T_c. As Van Vleck wrote [23], Weiss's approach is "qualitatively right but quantitatively wrong and is based half on theory and half on the genius at empirical guessing."

B. Exchange interaction and quantum Weiss-Heisenberg theory

The way out of this discrepancy was found 20 years later in the framework of newly emergent quantum mechanics. In 1926, Heisenberg explained that, in addition to the magnetic dipole-dipole coupling, a much stronger coupling of Fermi particles—electrons—of electrostatic Coulomb nature exists [24]. In quantum mechanics, the wave function Ψ of two identical electrons must be antisymmetric. Therefore, when the spins are parallel, the coordinate part of the Ψ function will also be antisymmetric, while for antiparallel spins it will be symmetric. This difference in symmetry of the coordinate function Ψ leads to distinct spatial distribution of the two electrons, resulting in a variation in their Coulomb energy, termed by Heisenberg the exchange energy [21,24]. He proposed a straightforward form of exchange energy E_{ij}^{ex} between two localized spins $\boldsymbol{S}_i$ and $\boldsymbol{S}_j$ at lattice points $\boldsymbol{R}_i$ and $\boldsymbol{R}_j$:

$$E_{ij}^{ex} = -J_{ij}\boldsymbol{S}_i \cdot \boldsymbol{S}_j. \tag{5a}$$

Here J_{ij} is the so-called exchange integral. Total exchange energy in the lattice E_{ex} reads

$$E_{ex} = -\frac{1}{2}\sum_{i,j} J_{ij}\boldsymbol{S}_i \cdot \boldsymbol{S}_j. \tag{5b}$$

Factor $1/2$ accounts for each particular contribution in (5a) appearing in (5b) twice.

The magnetic moment of Eu^{+2} originates from very localized $4f$ electrons with total spin $S = 7/2$ and magnetic moment $\mu = 2S\mu_B$. In the quantum era, to compute $\langle M(T)\rangle$ we have to account for a discrete series of spin orientations rather than a continuous distribution, as in the classical Langevin theory. With this modification, we have replaced the Langevin function $L(x)$ in (3a) by the so-called Brillouin function

$$\begin{aligned}\mathcal{B}_s(x) &= \frac{2S+1}{2S}\coth\left(\frac{2S+1}{2S}x\right) - \frac{1}{2S}\coth\left(\frac{x}{2S}\right)\\ &= \frac{(1+S)x}{3S} + [1-(1+2S)^4]\frac{x^3}{720S^4} + \cdots.\end{aligned} \tag{6a}$$

Now (3a) is amended as follows:

$$\begin{aligned}M(T) &= M_0 B_s[\mu(H + g_{ex}M)/T], \quad \mu = 2S\mu_B,\\ g_{ex} &= \frac{J_0}{2N_{lat}\mu_B^2}, \quad J_0 = \sum_j J_{ij} = Z_1J_1 + Z_2J_2 + \cdots.\end{aligned} \tag{6b}$$

Here, the parameter g_{ex} originates from the exchange interaction (5a). J_0 is the zero Fourier component of the exchange integral; J_1 is the exchange integral between the nearest-neighbor (nn) sites; $Z_1 \equiv Z$ is the nn coordination number (the number of nn pairs); J_2 is the next-nearest-neighbor (nnn) integral; and Z_2 is the nnn coordination number.

The exchange interaction in EuO and EuS occurs indirectly via more extended $5d$ wave functions [5]. Only two types of exchange interactions are important: J_1 and J_2; for their values, see Table I. The rest of the interactions can be peacefully neglected. Therefore, in (6b) for J_0, it is enough to account for only two terms. In fcc crystals, like EuO and EuS, $Z_1 = 12$ and $Z_2 = 6$; see Fig. 1. The lattice separations $\boldsymbol{R}_j = \boldsymbol{r}_{0,j}$ for the 12 nearest-neighbor sites and for the 6 next-nearest neighbors sites are

$$\begin{aligned}\boldsymbol{R}_1, \ldots, \boldsymbol{R}_{12} &= \left\{\pm\frac{a}{2}, \pm\frac{a}{2}, 0\right\}, \quad \left\{\pm\frac{a}{2}, 0, \pm\frac{a}{2}\right\},\\ &\quad \left\{0, \pm\frac{a}{2}, \pm\frac{a}{2}\right\};\\ \boldsymbol{R}_{13}, \ldots, \boldsymbol{R}_{18} &= \{\pm a, 0, 0\}, \quad \{0 \pm a, 0\}, \quad \{0, 0, \pm a\}.\end{aligned} \tag{7}$$

Here a is the size of the full cube in Fig. 1 consisting of four elementary cells of volume $v = a^3/4$ each.

It is convenient to rewrite (6b) in terms of $\overline{S}(T) \equiv \langle S\rangle_T$, introducing the so-called "normalized Brillouin function"

$$\begin{aligned}b_s(x) &= S\mathcal{B}_s(Sx)\\ &= \left(S+\frac{1}{2}\right)\coth\left(S+\frac{1}{2}\right)x - \frac{1}{2}\coth\left(\frac{x}{2}\right).\end{aligned} \tag{8}$$

For small x,

$$\begin{aligned}b_s(x) &= \frac{S(S+1)x}{3} - \frac{Sx^3}{90}B + \cdots,\\ B &= 1 + 3S + 4S^2 + 2S^3.\end{aligned} \tag{9}$$

For $H = 0$, we come to the quantum WH equation

$$\overline{S}(T) = b_s\left[\frac{\overline{S}(T)J_0}{T}\right]. \tag{10}$$

Using expansion (6a) and Eq. (6b) for g_{ex}, we find a new equation for the WH temperature T_c similar to (3c), but now accounting for the exchange interaction (5b):

$$T_c^{th} = \frac{2S(S+1)N_{lat}\mu_B^2 g_{ex}}{3S} = \frac{S(S+1)}{3}J_0. \tag{11a}$$

Temperature dependence of the magnetization (or mean spin $\overline{S}$) near T_c is also similar to (4a), but with a different prefactor

$$\overline{S} = \sqrt{\frac{T_c}{T} - 1}\sqrt{\frac{90}{SB}}\left(\frac{T}{J_0}\right)^{3/2}. \tag{11b}$$

For $T \approx T_c$, this relation may be approximated as

$$\overline{S} \approx \sqrt{T_c - T}\sqrt{\frac{90}{SB}}\frac{T_c}{J_0^{3/2}} \propto \sqrt{T_c - T}, \tag{11c}$$

corresponding to the scaling behavior of the order parameter $\overline{S} \propto (T_c - T)^{\beta_{MFA}}$ with the "normal" scaling exponent $\beta_{MFA} = 1/2$ predicted by the Landau theory of the second-order phase transitions [21] in general and MFA in particular.

Taking exchange integrals from Table I and using (6b), we obtain $J_0 \approx 16.5$ K for EuO and $J_0 \approx 4.1$ K for EuS. These further give $T_c^{th} \approx 86.6$ for EuO and $T_c^{th} \approx 21.4$ for EuS, which are not far from corresponding experimental values $T_c^{exp} \approx 69.2$ K for EuO and $T_c^{exp} \approx 16.6$ K for EuS.

The solution of Eq. (10) in the WH-MFA across the whole temperature range for EuO is shown in the main panel, and for EuS it is shown in the inset of Fig. 2(a) by a blue dotted line labeled (1). However, the agreement with the experiment is only qualitative. We conclude that the WH-MFA with the quantum-mechanical Heisenberg exchange interaction, Eq. (10), can serve as a leading-order approximation for the study of the thermodynamic properties of ferromagnetics.

Further efforts to improve the WH-MFA took into account larger clusters. In the paramagnetic phase (above T_c), their equilibrium dynamics were rigorously studied by Chertkov and Kolokolov [25,26]. Below T_c, larger clusters were studied, e.g., by Chamberlin [27]. However, due to divergence of the correlation length in the proximity of T_c, very large clusters are required to achieve the desired precision, resulting in minimal or no computational benefits compared to the evaluation of the whole system.

It is crucial to recognize that the methods mentioned above are unsystematic, making it difficult to control the nature of the assumptions and calculate corrections regularly. This issue can be resolved by using perturbation theory with graphical notation for the terms, known as the diagrammatic technique.

The details of the DT usage are too complex for the general reader, as it is geared towards experts in theoretical physics. Therefore, we placed our derivation of required corrections to the MFA in Appendix, where the interested reader will find all the technical details of the theory. The main physical results of Appendix are collected and thoroughly discussed in Sec. III, where we describe the consistent step-by-step improvements of the WH-MFA, culminating in an accurate quantitative description of the temperature dependence of magnetization throughout the entire temperature range from $T = 0$ to $T \lesssim T_c$. These findings are in excellent agreement with experimental results for EuO and EuS.

III. BEYOND THE QUANTUM WEISS-HEISENBERG MFA

In this section, we describe systematic, step-by-step corrections to WH-MFA, we analyze them in various limiting cases, and we explain the physical mechanisms behind the improved description of $M(T)$.

Note that both Weiss and Weiss-Heisenberg MFA replace the actual, time-dependent effective magnetic field $H_i(t)$ acting on some spin S_i with its mean value $H = \overline{H_i(t)}$, completely neglecting the fluctuations of the surrounding spins $S_j(t)$. The $\delta M(T)$ due to fluctuations are relatively small with a smallness parameter $1/Z$, where $Z = 12$ is the coordination number in EuO and EuS. The initial step to improve WH-MFA is described in Sec. III A, where fluctuations are considered in the first order of perturbation theory with respect to $1/Z$. This allows us to correctly describe the power-like decay of $M(T)$ for $T \ll T_c$ caused by spin waves instead of the incorrect exponential decay of $M(T)$ in the WH-MFA.

Nevertheless, the behavior of $M(T)$ near T_c is still not corrected sufficiently and gives the same T_c as the initial WH-MFA. This problem is addressed in the subsequent sections: III B and III C. The effect of long-propagating spin waves on the fluctuations of $H_i(t)$ is described more accurately by considering the exact kinematic identities (22), which connect all projections of the spin operator $\widehat{\boldsymbol{S}}$. This approach improved the behavior of $M(T)$ not only in the low-temperature range but also near the temperature T_c, including the value of T_c itself.

In the final Sec. III D, we combine two types of corrections to get the accurate quantitative description of $M(T)$ in the entire temperature range from $T = 0$ to T_c.

A. $\frac{1}{Z}$ corrections to the Weiss-Heisenberg MFA

The perturbation theory in $1/Z$ works well if the $\delta M(T)$ due to fluctuations of the magnetic fields are small compared to the mean value $M(T)$. Unfortunately, the fluctuations of the effective magnetic field $H_i(t)$ on a given spin S_i are relatively small with respect to their mean value H only when $T \ll T_c$. As T approaches T_c, H vanishes. In this case, the $H_i(t)$ fluctuations become larger compared to H, even in the first order in $1/Z$. This is a common problem in the theory of second-order phase transitions. First attempts in this direction, even using the diagrammatic perturbation approaches, faced serious problems: the VLP perturbation approach leads to infinite values of $1/Z$ corrections when $T \to T_c$ (for more details, see Appendix 1). As is elaborated in Appendix 3, we use a more sophisticated version of DT based on a generation functional. In our version of DT, $1/Z$ corrections are introduced in a much more compact form of a one-loop effective potential, described in Appendix 4. The resulting equations with the first-order in $1/Z$ corrections are as follows:

$$\begin{aligned}
&\overline{S} = A_0 + A_1 + A_2 + A_3,\\
&A_0 = b_s(\beta J_0 \overline{S}), \quad A_1 = A_{1a} + A_{1b}, \quad \beta = 1/T,\\
&A_{1a} = -\langle n_{\boldsymbol{k}} \rangle_{\boldsymbol{k}} = -\mathcal{N},\\
&A_{1b} = \langle n_0(\beta \overline{S} J_0) \rangle_{\boldsymbol{k}} = [\exp(J_0 \overline{S}/T) - 1]^{-1},\\
&A_2 = \beta b_S'(\beta J_0 \overline{S}) \langle J_{\boldsymbol{k}} n_{\boldsymbol{k}} \rangle_{\boldsymbol{k}},\\
&A_3 = \frac{\beta b_S''(\beta J_0 \overline{S})}{2} \left\langle \frac{\beta J_{\boldsymbol{k}}}{1 - \beta J_{\boldsymbol{k}} b_S'(\beta J_0 \overline{S})} \right\rangle_{\boldsymbol{k}}.
\end{aligned} \tag{12}$$

Here

$$\langle f_{\boldsymbol{k}} \rangle_{\boldsymbol{k}} \equiv \frac{v}{(2\pi)^3} \int f_{\boldsymbol{k}}\, d^3k, \quad \langle 1 \rangle_{\boldsymbol{k}} = 1, \tag{13}$$

which can be interpreted as the mean value of some function $f_{\boldsymbol{k}}$ per magnetic site, v is the unit-cell volume, and integration in Eq. (13) over $\boldsymbol{k}$ is carried out in the first reduced Brillouin zone for the wave vectors.

In Eq. (12), $b_s'(x) = db_s/dx$ and $b_s''(x) = d^2 b_s/dx^2$ are the first and second derivatives of the normalized Brillouin function $b_s(x)$ given by (8), and $\mathcal{N}$ is the mean value of the magnon numbers $n_{\boldsymbol{k}}$ per magnetic site, given by the Bose-Einstein distribution

$$\begin{aligned}
n_{\boldsymbol{k}} &= \left[\exp \frac{E_{\boldsymbol{k}}(T)}{T} - 1 \right]^{-1},\\
E_{\boldsymbol{k}}(T) &= \overline{S}_z(T)(J_0 - J_{\boldsymbol{k}}),\\
J_{\boldsymbol{k}} &= \sum_j J_{ij} \exp(i\boldsymbol{k} \cdot \boldsymbol{R}_{ij}).
\end{aligned} \tag{14}$$

Here $E_k(T)$ is "self-consistent" energy of spin waves, which can be found in the simplest version of the Green's function

splitting suggested by Tyablikov [28]. To rationalize this result from a physical point of view, at least for small $ak \ll 1$ and final temperatures, note that in these conditions, the main contribution to the decrease in $\overline{S}_z$ comes from the fast spin waves with $ak \sim 1$. This allows us to average the spin system over fast motions and to consider slow spin waves with $ak \ll 1$, as in the limit $T \to 0$, by replacing S (in our case $S = 7/2$) with $\overline{S}_z(T)$.

Note that Eqs. (12), considered as a straightforward expression for $1/Z$ corrections, are divergent at $T \to T_c$. However, if we consider (12) as self-consistent equations for $\overline{S}$, the divergencies are resolved because this procedure corresponds to a partial summation of the most divergent corrections in all orders in $1/Z$, similarly to Dyson resummation for the Green's functions in many versions of the diagrammatic perturbation approaches.

For actual calculations in EuO and EuS, we need explicit expressions for $J_0 - J_{\boldsymbol{k}}$ in these crystals. From (14) and (7), we find

$$\begin{aligned} J_0 - J_{\boldsymbol{k}} = 4J_1\Bigg[&\sin^2\frac{(k_x+k_y)a}{4} + \sin^2\frac{(k_x-k_y)a}{4} \\ &+ \sin^2\frac{(k_x+k_z)a}{4} + \sin^2\frac{(k_x-k_z)a}{4} \\ &+ \sin^2\frac{(k_y+k_z)a}{4} + \sin^2\frac{(k_y-k_z)a}{4}\Bigg] \\ &+ 4J_2\left[\sin^2\frac{k_x a}{2} + \sin^2\frac{k_y a}{2} + \sin^2\frac{k_z a}{2}\right]. \end{aligned} \tag{15}$$

1. Low-temperature spin-wave-dominated regime A

In the limit $T \to 0$, the term A_0 in Eqs. (12) gives the expected trivial answer $\overline{S} = S$. Together with the term A_{1a}, it gives a well-known result (cf. [17]) for the spin-wave correction of low-temperature mean spin,

$$\overline{S} \approx S - \mathcal{N}(T). \tag{16}$$

To estimate $\mathcal{N}(T)$, note that at small T, say for $T < 10$ K in EuO, the integral in $\langle n_{\boldsymbol{k}}\rangle$ is dominated by small k and the upper limit can be expanded to ∞. In cubic crystals, for small k,

$$E_{\boldsymbol{k}}(T) = E_{\rm ex}(ak)^2. \tag{17a}$$

For example, for EuO and EuS [according to (14) and (15)],

$$E_{\rm ex} = \overline{S}_z(T)(J_1 + J_2). \tag{17b}$$

This allows us to integrate $\langle n_k\rangle$ over angles in spherical coordinates and, finally, to come to a one-dimensional integral

$$\int_0^\infty \frac{x^2 dx}{\exp x^2 - 1} = \frac{\sqrt{\pi}}{4}\zeta(3/2) \approx 1.579.$$

Then $\mathcal{N}(T)$ can be estimated as

$$\mathcal{N}(T) \approx \frac{\zeta(3/2)}{32(\pi)^{3/2}}\left(\frac{T}{E_{\rm ex}}\right)^{3/2}. \tag{18}$$

Using J_1, J_2 from Table I in Eq. (17b), we obtain the values of $E_{\rm ex} \approx 1.50$ K for EuO and $E_{\rm ex} \approx 0.22$ K for EuS.

In the limit $T \to 0$, the rest of the terms in (12) give exponentially small corrections:

(i) Term $A_{1b} \approx \exp(-J_0 S/T)$.

(ii) Term $A_2 \approx \exp(-J_0 S/T)\mathcal{N}$, where $\mathcal{N} \propto T^{3/2}$; see (18).

(iii) Term $A_3 \approx \frac{\langle J_{\boldsymbol{k}}\rangle_{\boldsymbol{k}}}{2T}\exp\left(-\frac{J_0 S}{T}\right)$, where $\langle J_{\boldsymbol{k}}\rangle_{\boldsymbol{k}}$ is defined by Eq. (14).

Therefore, our result, Eqs. (12), gives an expected and well-known low-temperature behavior (for $T \lesssim 40$ K in EuO) of $\overline{S}(T)$; see, for example, [17].

2. Near-T_c behavior of $\frac{1}{Z}$-corrected MFA

In the critical regime C, the spin fluctuations dominate the magnetization behavior, and even the corrected MFA is no longer valid. Nevertheless, its analysis is still instructive, allowing us to find the estimate of T_c in this approximation.

To find the behavior of the magnetization in the limit $\overline{S} \to 0$, we consider the basic equations (12) with $n_{\boldsymbol{k}}$ given by Eqs. (14). Here, we can use the Rayleigh-Jeans distribution

$$n_{\boldsymbol{k}} = \frac{T}{E_{\boldsymbol{k}}} \Rightarrow \frac{T}{\overline{S}(J_0 - J_{\boldsymbol{k}})}, \quad n_0(x) \Rightarrow \frac{T}{\overline{S}J_0}. \tag{19}$$

Using the expansions of (9) for $x = J_0\overline{S}/T \ll 1$, we can simplify equations for A_j accounting for terms of order of $x^{\pm 1}$, denoted as $A_j^{\pm 1}$:

$$\begin{aligned} A_0^{(1)} &= \frac{S(S+1)}{3}\frac{\overline{S}J_0}{T} = \overline{S}\frac{T_c}{T}, \\ A_1^{(-1)} &= -\frac{T}{\overline{S}J_0}\left\langle\frac{J_k}{J_0 - J_k}\right\rangle, \quad A_1^{(1)} = 0, \\ A_2^{(-1)} &= \frac{S(S+1)}{3\overline{S}}\left\langle\frac{J_k}{J_0 - J_k}\right\rangle, \\ A_2^{(1)} &= -\frac{BJ_0^2\overline{S}}{T^2}\left\langle\frac{J_k}{J_0 - J_k}\right\rangle, \\ A_3^{(1)} &= -\frac{SB}{15}\frac{J_0\overline{S}}{T}\left\langle\frac{J_k}{T - J_k S(S+1)/3}\right\rangle \\ &\approx \frac{BJ_0\overline{S}}{5(S+1)}\left\langle\frac{J_k}{J_0 - J_k}\right\rangle. \end{aligned} \tag{20}$$

Here, averaging $\langle\cdots\rangle$ is understood according to (13).

We see that in the limit $\overline{S} \to 0$, the terms $A_1^{(-1)}$ and $A_2^{(-1)}$ diverge as $1/\overline{S}$. However, the sum of these two terms,

$$A_1^{(-1)} + A_2^{(-1)} = \left\langle\frac{J_k}{J_0 - J_k}\right\rangle\frac{1}{\overline{S}}\left[\frac{S(S+1)}{3} - \frac{T}{J_0}\right] \propto \frac{T_c - T}{\overline{S}},$$

behaves as $\overline{S}$ near Curie temperature (11a), $T_c = S(S+1)J_0/3$, under the assumption that $\overline{S} \propto \sqrt{T_c - T}$.

To verify this assumption, consider Eq. (12) with approximate values of A_j given by (20). To simplify the appearance of the resulting (21), we multiply each term by $\overline{S}$, divide by $\langle\frac{J_k}{J_0 - J_k}\rangle$, and rearrange to get

$$\frac{BJ_0\overline{S}^2}{T(S+1)}\left[\frac{3}{S} + \frac{1}{5(S+1)}\right] = \frac{T_c - T}{J_0}. \tag{21}$$

Here we note that $\overline{S}^2 - \overline{S}A_0^{(1)}$ is proportional to $\overline{S}^2(T_c - T) \propto \overline{S}^4$, and we neglect it in (21). Terms $A_2^{(1)}$ and $A_3^{(1)}$ contribute

to the left-hand side (LHS) of Eq. (21), while $A_1^{(-1)}$ and $A_2^{(-1)}$ contribute to its right-hand side (RHS).

In particular, we observe that as T approaches the critical temperature T_c, the order parameter $\overline{S}$ behaves as $\overline{S} \propto \sqrt{T_c - T}$. This demonstrates that within the $1/Z$-corrected MFA, the scaling behavior of the order parameter is $\overline{S} \propto (T_c - T)^{\beta_{\rm MFA}}$, with the normal scaling exponent $\beta_{\rm MFA} = \frac{1}{2}$. Furthermore, the $1/Z$ corrections to the original quantum MFA do not alter the critical temperature T_c as given in the original Eq. (11a). These corrections only affect the prefactor, which now differs from that in Eq. (11b).

3. Numerical solution of Eq. (12)

The numerical solution of Eq. (12), shown in Fig. 2(a) by the solid blue line, is compared to the solutions of the Weiss-Heisenberg Eq. (10) (dotted blue line) and the experimental results for EuO. It is observed that the solution of the mean-field equation $\overline{S} = b_s(\beta J_0 \overline{S})$ deviates significantly from the experiment (solid black line with circles) in the entire temperature range. At the same time, the solution of the $1/Z$-corrected Eq. (12) (represented by the solid blue line) offers an accurate quantitative description of the experiment in the low-temperature region ($T \lesssim 60$ K for EuO), dominated by spin-wave contribution. However, this solution deviates significantly from the experiment for larger temperatures.

A way to resolve this problem, demonstrating very accurate qualitative agreement between the developed theory and experiment, is shown below.

B. Nonequilibrium Belinicher-L'vov DT for spin operator

The essential progress in this area was made by Belinicher and L'vov (BL), who developed a diagrammatic technique for spin operators [20] using graphical notations similar to those traditionally employed in Feynman's diagrammatic technique. BL extended Keldysh's diagrammatic technique to nonequilibrium Bose systems for the case of spin operators. The key element here was the formulation of Wick's theorem for spin operators, which allows the expression of the mean values of the product of any number of spin operators,

$$\widehat{S}_\pm = (\widehat{S}_x \pm i\widehat{S}_y)/\sqrt{2} \quad \text{and} \quad \widehat{S}_z,$$

through products of only operators S_z. The BL-DT explicitly incorporates the mean values of the spin-wave propagators (expressed via $\widehat{S}_\pm$), while the longitudinal correlation functions of $\widehat{S}_z$ play a role as external parameters characterizing the media in which the spin waves propagate. Calculating longitudinal correlations is a nontrivial task. One way to achieve this is to formulate a perturbation approach starting from the basic WH-MFA in which there is no mention of spin waves. With this starting point, one has to account in any order of perturbation approach for the fulfillment of the kinematic identities

$$\widehat{\boldsymbol{S}}^2 = -2\widehat{S}_+\widehat{S}_- + \widehat{S}_z^2 - \widehat{S}_z = S(S+1), \tag{22}$$

which provides a connection between dynamic operators $\widehat{S}_\pm$ and powers of the static ones, $\widehat{S}_z$.

In BL-DT kinematic identities, Eq. (22) is used from the start to express correlations $\langle \widehat{S}_z^n \rangle$ as polynomials of $\widehat{S}_\pm$. These correlations can be calculated using the longitudinal part of the DT. This approach allows for an efficient calculation method in which even a single simple diagram considered corresponds to the summation of a series of several diagrams in the framework of the Vaks-Larkin-Pikin approach.

C. Spin-waves-improved Weiss-Heisenberg MFA

BL showed that accounting for kinematic identities (22) in the leading-order approximation in $1/Z$ leads to the following modification of MFA:

$$\overline{S}_z(T) = b_s(y), \; y = \ln\left(1 + \frac{1}{\mathcal{N}}\right), \tag{23}$$

where $\mathcal{N} = \langle n_{\boldsymbol{k}} \rangle_{\boldsymbol{k}}$, the mean value of the occupation numbers, is the free parameter of the problem. Its value depends on real physical conditions: in the case of strong external pumping, it can be found from the wave kinetic equations. In thermodynamic equilibrium, $n_{\boldsymbol{k}}$ is determined by the Bose-Einstein distribution (14).

In thermodynamic equilibrium, Eqs. (23) were suggested by Praveczki [29] for $S \leqslant 3.0$ (recall that in EuO and EuS, $S = 7/2$), and they were accounting only for nearest-neighbor interactions; see also [28,30,31].

Equations (23) can be rewritten in a form more closely resembling the original version (10) of the quantum MFA:

$$\overline{S}_z(T) = b_s\left[\frac{E_{\rm eff}(T)}{T}\right], \tag{24a}$$

$$\left[\exp\frac{E_{\rm eff}(T)}{T} - 1\right]^{-1} = \left\langle\left[\exp\frac{E_{\boldsymbol{k}}(T)}{T} - 1\right]^{-1}\right\rangle,$$

$$E_{\boldsymbol{k}}(T) = \overline{S}_z(J_0 - J_{\boldsymbol{k}}). \tag{24b}$$

Here, we replace $\overline{S}(T)J_0$ in Eq. (10) with the effective energy on the site $E_{\rm eff}(T)$ defined by Eq. (14). In a way, $E_{\rm eff}(T)$ can be considered as a sophisticated mean value of the spin-wave energy $E_{\boldsymbol{k}}(T)$ over the entire $\boldsymbol{k}$-space at a given T. We consider Eq. (24) to be physically motivated and more transparent than its original form (23).

As is shown below, Eq. (23) [or, equivalently, Eq. (24)] is significantly more accurate than the corresponding Eq. (10) for WH-MFA and even Eqs. (12) describing WH-MFA with $1/Z$-corrections.

1. $\overline{S}_z(T)$ in low-T regime A

When $T \to 0$, $\mathcal{N}$ is very small and $y \gg 1$ in (23). In that case,

$$\overline{S}_z(T) \approx S - \frac{\mathcal{N}(T)}{1 + \mathcal{N}(T)} \approx S - \mathcal{N}(T), \tag{25}$$

i.e., as anticipated, the decrease in $\overline{S}_z(T)$ is precisely governed by the excitation of spin waves [17]. Note that Eq. (25) coincides with Eq. (16) for $\overline{S}_z(T)$ in the "original" mean-field approximation with $1/Z$ corrections.

2. $\overline{S}_z(T)$ in precritical regime B

Let us show that the temperature dependence $\overline{S}_z(T)$ in the spin-wave-improved mean-field approximation, considered here and in the "original" mean-field, $1/Z$-corrected

approximation, is very different when T approaches T_c, the mean spin $\overline{S}_z(T) \to 0$, and the energy $E_{\boldsymbol{k}}(T)$ in (24a) also approaches zero and become much smaller than T. In that case, the Bose-Einstein distribution (24b) can be approximated by the Rayleigh-Jeans distribution $T/E_{\boldsymbol{k}}(T)$, and Eq. (24b) reduces to

$$E_{\rm eff} = \overline{S}\widetilde{J}_0. \tag{26a}$$

Here, we introduce the effective exchange integral, defined as follows:

$$\frac{1}{\widetilde{J}_0} \equiv \left\langle \frac{1}{J_0 - J_{\boldsymbol{k}}} \right\rangle_{\boldsymbol{k}}. \tag{26b}$$

We observe that Eqs. (24a) and (26a) coincide with the original mean-field Eq. (10) after replacing $\widetilde{J}_0$ with J_0. This means that in the spin-wave-improved MFA $\overline{S}_z$ vanishes at the new value of the Curie temperature,

$$\widetilde{T}_c = \frac{S(S+1)\widetilde{J}_0}{3} = \frac{S(S+1)}{3}\left\langle \frac{1}{J_0 - J_k} \right\rangle^{-1}, \tag{26c}$$

and in its vicinity it behaves as a square root of the temperature difference, similarly to (4a):

$$\overline{S} = C\sqrt{\frac{\widetilde{T}_c - T}{\widetilde{T}_c}}, \quad C = \frac{1}{S}\sqrt{\frac{3}{B(S+1)^3}}, \tag{26d}$$

where B is defined by (9), and C depends only on S. As is evident from Eq. (26d), the scaling behavior near the Curie temperature within the spin-wave-improved MFA remains normal, $\beta_{\rm MFA} = 1/2$. However, the Curie temperature, denoted as $\widetilde{T}_c < T_c$, is now determined by the effective exchange integral $\widetilde{J}_0$, which is smaller than the "bare" exchange integral J_0. The ratio $\widetilde{T}_c/T_c \approx 0.77$ in EuO and $\widetilde{T}_c/T_c \approx 0.64$ in EuS. The physical reason for this improvement is the suppression of the longitudinal correlations of spins due to the excitation of spin waves in the vicinity of T_c, as is reflected by kinematic identities (22).

3. *Numerical solution of Eq. (23) and its analysis*

The numerical solution of the spin-wave-improved WH-MFA, Eq. (23) for $\overline{S}_z(T)$ in EuO, is shown in Fig. 2(a) by the dashed green line labeled (3). It is interesting to compare this behavior with the similar curve of $\overline{S}_z(T)$ in the $1/Z$-corrected WH-MFA, Eq. (12), plotted in Fig. 2(a) by the solid blue line labeled (2). We showed analytically that in both approximations, the low-T behavior is the same: $\overline{S}_z \approx S - \mathcal{N}(T)$. Consequently, both curves practically coincide for $T \lesssim 20$ K, and they remain quite close for temperatures up to $T \simeq 50$ K. However, for larger T these curves deviate significantly: the solid blue line for the $1/Z$-corrected MFA goes to zero at $T_c \approx 86.6$ K, while the dashed green line for the spin-wave-improved MFA approaches zero at $\widetilde{T}_c \approx 66.5$ K, which is much closer to the experimental value $T_c^{\rm exp}$ in EuO.

We conclude that the spin-wave-improved MFA captures physics better than its $1/Z$-corrected counterpart for $T > T_c/2$. We tend to associate this difference with the kinematic identities, (22), that relate the dynamic operators $\widehat{S}_\pm$ to the static ones $\widehat{S}_z$ on the same site. In the original WH-MFA, an interaction of a spin on a given site with its real environment with fluctuating spins is approximated by its interaction with the mean values of surrounding spins, producing a time-independent magnetic field $H_{\rm eff} = \overline{S}_z J_0$. In thermodynamic equilibrium, this field causes a nonzero value of $\overline{S}_z/S$, given by the normalized Brillouin function b_s according to (10). However, in the presence of intense spin waves, this is not the case: according to kinetic identities, when $\langle \widehat{S}_+ \widehat{S}_- \rangle \neq 0$, the mean spin $\overline{S}_z$ cannot reach its maximal value S and vanishes for smaller T, i.e., faster than without accounting for the spin waves.

D. $1/Z$ corrections to the spin-wave-improved mean-field equation and its analysis

Using the spin-wave-improved mean-field equation, Eq. (23), as a leading-order approximation, and finding the required first-order corrections in $\frac{1}{Z}$, we obtain the following version of the self-consistent equation for $\overline{S}$:

$$\overline{S} = \widetilde{A}_0 + \widetilde{A}_1 + A_2 + A_3, \tag{27a}$$

$$\widetilde{A}_0 = b_s(y), \quad y = \ln\left(1 + \frac{1}{\mathcal{N}}\right), \tag{27b}$$

$$\widetilde{A}_1 = \left[1 - \frac{b_s'(y)}{\mathcal{N}(\mathcal{N}+1)}\right] A_1. \tag{27c}$$

Here A_1, A_2, A_3, and $\mathcal{N}$ are given by Eq. (12). Equation $\overline{S} = \widetilde{A}_0$ coincides with the spin-wave-improved mean-field equation (24). As we have shown, it gives for $T \to 0$ the spin-wave correction $\overline{S} = S - \mathcal{N}$. The same correction gives the term A_1 in Eq. (12). The prefactor in Eq. (27c) vanishes for $T \to 0$ to prevent double counting of the spin-wave correction.

Note that analysis of near-T_c behavior of $\overline{S}(T)$ in the framework of Eqs. (20) for $1/Z$ corrected WH-MFA shows that $\overline{S}(T) = 0$ at $T_c = S(S+1)J_0/3$. This follows from the balance of A_1, A_2, and A_3 terms in (21). The analytical equations for these terms in (27) are the same as in Eqs. (12) and (20). Therefore, it is not surprising that $\overline{S}(T) \to 0$ for $T \to T_c$ and not for $T \to \widetilde{T}_c$. The reason is that we derived the equations for A_j in the framework of DT developed in Appendixes 3 and 4, which ignores kinematic identities. The straightforward way to account for them is to derive A_j in the framework of the BL DT.

Unfortunately, this is quite a cumbersome procedure. Instead, we observe that in the range where $\overline{S} \ll S$, spin waves suppress the effective exchange integrals by a factor of $R \equiv \widetilde{J}_0/J_0$. Therefore, in all expressions for A_j, we replace J_0 by $\widetilde{J}_0$ and $J_{\boldsymbol{k}}$ by $RJ_{\boldsymbol{k}}$. Modified in this way, Eqs. (27) for the $1/Z$-corrected, spin-wave-improved MFA for $\overline{S}_z/S(T)$ were solved numerically with EuO parameters and shown in Fig. 2(a) by a solid green line. The accuracy of the numerical solution decreases as $\overline{S}$ becomes smaller. We cannot guarantee its reliability when $S(T) < 0.1\overline{S}$.

Therefore, we did not plot the numerical solution for $S(T)$ in this T-range.

We see further improvement of the result in comparison with the uncorrected spin-wave-improved mean-field equation (24), plotted in Fig. 2(a) by the dashed green line.

When the small discrepancy in the Curie temperature values is compensated by plotting in Fig. 2(b) $\overline{S}_z/S$ versus normalized temperature T/T_c, the theoretical curves of $\overline{S}_z/S$ in the $1/Z$-corrected spin-wave-improved MFA almost coincide with experimental results for EuO and EuS.

Another impressive result is observed in Fig. 2. We approximated the numerical solution of Eqs. (27), $\overline{S}_z/S$ [accurate for $S(T) \gtrsim 0.1\overline{S}$], by a power-law-like T-dependence $(1 - T/T_c)^{\beta_*}$ in the temperature range corresponding to $0.1\overline{S} < S(T) < 0.6\overline{S}$. This dependence is plotted in Fig. 2 by the solid red line in the wider T-range including $T = \widetilde{T}_c$, where $S(T) = 0$. The value of the apparent precritical anomalous scaling index $\beta_* = 0.34 \pm 0.02$ is in excellent agreement with its experimental value $\beta_{\rm exp} = 0.36 \pm 0.01$ in EuO and EuS [10]. Note that the experimental scaling index was measured by fitting $S(T)$ in the $(T_c - T)/T_c \lesssim 0.11$ range. Therefore, the experimental value $\beta_{\rm exp} = 0.36 \pm 0.01$ corresponds to the precritical regime B.

It is noteworthy that β_* and $\beta_{\rm exp}$ are also quite close to the theoretical critical exponent $\beta_{\rm cr} \approx 0.365$, deduced within the renormalization-group theory for the 3D Heisenberg ferromagnet, particularly suitable in the critical regime C [12]. While it is not entirely clear why β_* and $\beta_{\rm cr}$ are so similar, the extended tail of critical scaling in the precritical regime may be attributed to the particular way we treat the $1/Z$ corrections to MFA. Within the spin-wave-improved Weiss-Heisenberg MFA, we consider exact kinematic identities (22), which incorporate complete perturbation series rather than just first in $1/Z$ terms. Moreover, as was mentioned above, we solve (27) self-consistently. This process is akin to Dyson's resummation of (presumably) the most divergent terms. It is plausible that the described dual resummation of infinite diagrammatic series captures the key contributions from longitudinal and transversal spin fluctuations, thus extending the scaling from the critical to the precritical regime. Experimental observations matching the extended precritical anomalous scaling lend additional support for this conjecture and the importance of the introduced corrections for the description of basic physical mechanisms defining magnetization.

IV. SUMMARY

In this paper, we revisited the theoretical description of spontaneous magnetization in cubic ferromagnetic crystals. Using a consistent two-step procedure based on the diagrammatic technique, we developed a theory that accounts for intensive and long-propagating spin waves—fluctuations of the transverse spin components. Our theory resolves the long-standing problem of accurate quantitative description of the temperature dependence of magnetization in cubic ferromagnetic crystals.

We explain the physical reasons for the failure of other approaches, and we demonstrate the step-by-step improvement in describing the temperature dependence of the spontaneous magnetization emerging in our method.

Our theoretical approach marks a significant advancement in the description of magnetic systems. Specifically, we theoretically identified a broad intermediate precritical regime B, situated between the low-temperature, spin-wave-dominated regime A and the critical $(T_c - T \ll T_c)$ regime C. In the precritical regime, $M(T)$ follows a scaling behavior $M(T) \propto (T_c - T)^{\beta_*}$, characterized by the precritical anomalous exponent $\beta_* \approx 1/3$.

Our approach is not limited to simple ferromagnets but may be extended to ferrimagnetic materials with multiple magnetic sublattices, such as yttrium-iron-garnet, and antiferromagnets that involve exchange and dipole-dipole interactions, as well as anisotropy energy, among other factors.

ACKNOWLEDGMENTS

We are grateful to E. Podivilov, A. Shafarenko, V. Cherepanov (now deseased), and V. Belinicher (now deseased) for their contributions in the preliminary stages of this work many years ago. The authors also thank A. Chumak for fruitful discussion. I.K. gratefully acknowledges the support of the Russian Ministry of Science and High Education. V.L. was partially supported through the Project No. I-6568 "Paramagnonics."

DATA AVAILABILITY

The data that support the findings of this article are not publicly available. The data are available from the authors upon reasonable request.

APPENDIX: DIAGRAMMATIC TECHNIQUE FOR HEISENBERG FERROMAGNETS

1. Vaks-Larkin-Pikin DT for spin operators in thermodynamic equilibrium

The initial formulation of the DT for ferromagnetic materials was proposed by Vaks, Larkin, and Pikin (VLP) [18,19]. Their DT, formulated for the thermodynamic equilibrium, produced important results. Later, Izyumov and Skryabin [32] and Bar'yakhtar, Krivoruchko, and Yablonski [17] adapted VLP DT for direct use with spin operators. These DTs have produced several noteworthy and crucial findings [17–19,32].

From the formal point of view, the WH mean-field Eq. (10) is the leading-order approximation in these approaches, valid in the limit of an infinitely large radius of interaction R, defined as follows:

$$R^2 = \sum_j R_{ij}^2 J_{ij}/a^2 J_0. \tag{A1}$$

VLP also computed first-order corrections in R^{-3} for $M(T, H)$ in (6b) and the simultaneous spin-correlation functions. According to [18], the expansion parameters of this theory for the cubic, body-centered-cubic (bcc), and fcc lattices with nearest-neighbor interactions are 1, $2^{-3/2} \approx 0.35$, and $3^{-3/2} \approx 0.19$, respectively. However, since exchange interactions decay rapidly with distance, the theory, in its original formulation, is formally inappropriate for most ferrodielectrics.

Most of the results obtained in this DT [17–19,32] have not gained widespread acceptance, both because of the specific difficulties inherent in these diagram techniques and the unsuccessful graphical notation, which makes it difficult to establish analogies and perceive the information presented.

Note also that in the VLP approach, the corrections to $M(T)$ become infinite as T approaches T_c. This behavior is not physical because $0 < M(T) < M_0$. Therefore, it is necessary to reformulate the theory to eliminate these infinite values. This is done below in Appendixes 2, 3, and 4, where we provide a regularized theory that describes corrections to

quantum WH-MFA that are applicable over a wider range of temperatures.

2. Physical small parameter

We have to note that from a physical point of view, MFA in ferromagnetics neglects the fluctuation of the effective magnetic field and becomes exact when the number of interacting magnetic atoms goes to infinity. For fcc crystals with nearest-neighbor interactions, this number is the coordinate number $Z_1 = 12$. Thus, the applicability parameter in this case is $1/Z_1 = 1/12$, which is much smaller than the formal expansion parameter $1/R^3 = 1$, declared by VLP. Moreover, when the next-nearest interactions are important, one has to account for their contribution to the exchange integral J_0. Thus we expect that in the general case, the role of coordinate number Z is played by $Z_{\rm eff} = J_0/J_1 \approx Z_1 + Z_2 J_2/J_1$. In EuO, $Z_{\rm eff} \approx 13.2$ while in EuS, $Z_{\rm eff} \approx 9.4$. This explains why we hope to reach a better agreement between an experiment and the mean-field approach for EuO than for EuS. Indeed, according to Table I, in EuO $[T_{\rm c}^{\rm ex} - T_{\rm c}^{\rm exp}]/T_{\rm c}^{\rm exp} \approx 0.24$ while in EuS this ratio is about 0.29.

3. Functional representation

In this paper, we are interested in the spontaneous magnetization $M(T)$, which is proportional to the mean spin $\overline{S}_z$, defined by (1) and aligned with the external magnetic field $\boldsymbol{h} = \{0,\ 0, h_z \equiv h\}$. Following [33,34], we compute $M(T)$ as

$$\overline{S}_z = \frac{T}{N_{\rm lat}} \frac{d}{dh} \ln \mathcal{Z}(h), \quad h \to 0 \tag{A2}$$

from the generating function

$$\mathcal{Z}(h) = \ {\rm Tr}\ \exp\left(-\beta \mathcal{H}_{\rm ex} + \beta h \sum_j S_j^z\right). \tag{A3}$$

Here, "Tr" represents the trace operator. The Heisenberg exchange Hamiltonian, denoted as $\mathcal{H}_{\rm ex}$, is derived from the exchange energy described in Eq. (5b), and it has the following form:

$$\mathcal{H}_{\rm ex} = -\frac{1}{2} \sum_{jk} J_{jk} \boldsymbol{S}_j \boldsymbol{S}_k, \tag{A4}$$

where $\boldsymbol{S}_j$ are spin operators at the lattice sites $\boldsymbol{R}_j$. To confine the operator problem to a single lattice site, the Hubbard-Stratonovich transformation [35,36] is utilized.

The noncommutativity of spin components prevents us from rewriting the partition function as an integral over vector variables defined on each lattice site. Instead, the fields dependent on artificial time emerge, leading to an expression involving functional integrals over these fields defined on the lattice.

First we represent $\mathcal{Z}(h)$ as an infinite product:

$$\mathcal{Z}(h) = \exp\left(-\epsilon \mathcal{H}_{\rm ex} + \epsilon h \sum_j S_j^z\right) \times \cdots \times \exp\left(-\epsilon \mathcal{H}_{\rm ex} + \epsilon h \sum_j S_j^z\right). \tag{A5}$$

Formally, we need to let ϵ approach 0, but for now, let us consider it as a very small but finite quantity. The number of terms in the product (A5) is β/ϵ. Then we use the identity valid in the limit $\epsilon \to 0$,

$$\exp\left(\frac{\epsilon}{2} J_{jk} \mathbf{S}_j \mathbf{S}_k\right) = \mathcal{M}_\epsilon \int \prod_j d\boldsymbol{\phi}_j \exp\left(-\frac{\epsilon}{2} J_{jk}^{-1} \boldsymbol{\phi}_j \boldsymbol{\phi}_k + \epsilon \boldsymbol{\phi}_j \mathbf{S}_j\right), \tag{A6}$$

where J_{jk}^{-1} is the inverse matrix of J_{jk}, and $\mathcal{M}_\epsilon$ is a normalization factor. Substituting it into (A5), we have for each lattice site j a set of integration variables corresponding to each multiplier in the product (A5). This set can be considered as a function $\boldsymbol{\phi}_j(t)$ defined in discrete time $t = 0, \epsilon, 2\epsilon, \ldots, \beta$. In a formal continuum limit, we obtain integral sums as an exponent and a product of time-ordered exponentials:

$$\mathcal{Z}(h) = \int \prod_l \mathcal{D}\boldsymbol{\phi}_l(\tau) \exp\left[-\frac{1}{2} \int_0^\beta J_{jk}^{-1} \boldsymbol{\phi}_j(\tau) \boldsymbol{\phi}_k(t)\, d\tau\right] \times \prod_j {\rm Tr\,T} \exp\left[\int_0^\beta d\tau (\boldsymbol{\phi}_j(\tau) + \boldsymbol{h}_j) \boldsymbol{S}_j\right]. \tag{A7}$$

The symbol T denotes a chronological product, and $\boldsymbol{h}_j = (0, 0, h)$. The path integral (A7) is understood as a limit of finite-dimensional approximations. The measure of integration is

$$\mathcal{D}\boldsymbol{\phi}_l(t) = \mathcal{M} \prod_{\alpha=x,y,z} \prod_{n=1}^{\beta/\epsilon} d\phi_l^\alpha(n\epsilon), \tag{A8}$$

where $\mathcal{M} = (\mathcal{M}_\epsilon)^{\beta/\epsilon}$.

Let us rewrite (A7) more conveniently by shifting the variables of functional integration $\boldsymbol{\phi} = \boldsymbol{\varphi} + \boldsymbol{h}$:

$$\mathcal{Z}(\boldsymbol{h}) = \int \prod_l \mathcal{D}\boldsymbol{\varphi}_l(\tau) \exp\left[-\frac{1}{2} \int_0^\beta J_{jk}^{-1} \boldsymbol{\varphi}_j(\tau) \boldsymbol{\varphi}_k(\tau) d\tau + \frac{h}{J_0} \int_0^\beta \sum_j \varphi_j^z(\tau) d\tau - N_{\rm lat} \frac{\beta h^2}{2J_0}\right] \times \prod_j {\rm Tr}\left[{\rm T} \exp\left(\int_0^\beta \boldsymbol{\varphi}_j(\tau) \boldsymbol{S}_j d\tau\right)\right]. \tag{A9}$$

The time-ordered operator exponent

$$\hat{A}(t) = {\rm T}\left\{\exp\left[\int_0^t \boldsymbol{\varphi}(\tau) \boldsymbol{S} d\tau\right]\right\} \tag{A10a}$$

is defined by the equation

$$d\hat{A}(t)/dt = [\boldsymbol{\varphi}(t) \boldsymbol{S}] \hat{A}(t) \tag{A10b}$$

with the initial condition $\hat{A}(0) = 1$. The operator $\hat{A}$ cannot be expressed explicitly as a functional of $\boldsymbol{\varphi}(t)$. However, there is a way to rewrite the T-ordered exponential as a product of regular ones. To demonstrate this, let us consider the operator

given as a product of the usual matrix exponential:

$$\widehat{\mathcal{A}}(t) = \exp[-S^+\psi^-(t)]\exp\left[S^z\int_0^t \rho(\tau)\,d\tau\right] \times \exp\left\{\frac{1}{2}S^-\int_0^t d\tau\psi^+(\tau)\exp\left[\int_0^\tau \rho(\tau')\,d\tau'\right]\right\} \times \exp[S^+\psi^-(0)]. \tag{A11}$$

Here, $S^\pm = S^x \pm iS^y$ and $\psi^\pm(t)$, $\rho(t)$ are some new fields. Using the commutators

$$\begin{aligned}
[S^-, F(S^+)] &= -2S^zF'(S^+) + S^+F''(S^+),\\
[S^z, F(S^-)] &= -S^-F'(S^-),\\
[S^+, F(S^-)] &= 2S^zF'(S^-) + S^-F''(S^-),\\
S^-F(S^z-1) &= F(S^z)S^-,
\end{aligned} \tag{A12}$$

where $F(y)$ is some function, one can be convinced that the operator $\hat{\mathcal{A}}(t)$ satisfies the following equation:

$$\frac{d\widehat{\mathcal{A}}}{d\tau} = \left\{[\rho - \psi^+\psi^-]S^z + \frac{1}{2}\psi^+S^- + [-\dot{\psi^-} + \rho\psi^- + \frac{1}{2}\psi^+(\psi^-)^2]S^+\right\}\hat{\mathcal{A}}(t). \tag{A13}$$

The last factor in (A11) provides the equality $\hat{\mathcal{A}}(0) = 1$. Considering the following change of variables in the functional integral over the measure,

$$\begin{aligned}
\varphi^z &= \rho - \psi^+\psi^-,\\
\varphi^- &= -\dot{\psi^-} + \rho\psi^- - \tfrac{1}{2}\psi^+(\psi^-)^2,\\
\varphi^+ &= \tfrac{1}{2}\psi^+, \quad \varphi^\pm = \tfrac{1}{2}(\varphi^x \pm i\varphi^y),
\end{aligned} \tag{A14}$$

we see that the T-ordered operator $\hat{A}(t)$, defined by Eqs. (A10), takes the form (A11):

$$\widehat{A}(t) = \widehat{\mathcal{A}}(t), \tag{A15}$$

without T-ordering. This allows us to obtain an explicit functional integral representation for any physical quantities of interest.

The change of variables (A14) contains the time derivative of ψ^- on the right-hand side. Hence, it is necessary to impose the boundary or initial conditions.

Here, we utilize the periodic boundary conditions typically used in the statistical physics of Bose systems. It is essential to calculate the Jacobian $\mathcal{J}$ considering the boundary conditions

$$\mathcal{J} = \text{const}\,\sinh\left(\frac{1}{2}\int_0^\beta \rho\,dt\right). \tag{A16}$$

The analyticity of the integrand and the convergence of the functional integral allow us to deform the initial surface of integration into a standard one: $\mathrm{Im}\rho = 0$, $\psi^+ = (\psi^-)^*$. In this way, the trace of the operator $\hat{\mathcal{A}}(\beta)$ (A11) can be easily calculated for an arbitrary value of the spin S:

$$\mathrm{Tr}[\widehat{\mathcal{A}}(\beta)] = \mathrm{Tr}[\hat{A}(\beta)] = \exp\left[\mathcal{Q}_s\left(\int_0^\beta \rho\,dt\right)\right]. \tag{A17}$$

Here $\mathcal{Q}_s(x)$ is a primitive of normalized Brillouin function b_s, given by (8):

$$\mathcal{Q}_s(x) = \ln\frac{\sinh[x(S+1/2)]}{\sinh(x/2)}, \tag{A18a}$$

$$b_s(x) = d\mathcal{Q}_s(x)/dx. \tag{A18b}$$

Note that $\mathcal{Q}(x)$ differs from the original Brillouin function $\mathcal{B}_s(x)$, given by (6a).

Thus, according to (A2), (A9), and (A14)–(A18), the spontaneous magnetization is given by the expectation value

$$\bar{S} = \frac{T}{N_{\mathrm{lat}}J_0}\left\langle\int_0^\beta \sum_j \varphi_j^z(\tau)d\tau\right\rangle = \frac{T}{N_{\mathrm{lat}}J_0}\left\langle\int_0^\beta \sum_j (\rho_j - \psi_j^+\psi_j^-)(\tau)d\tau\right\rangle \tag{A19}$$

with respect to the measure

$$\mathcal{D}\rho\mathcal{D}\psi^+\mathcal{D}\psi^-\exp\left[-\int_0^\beta \mathcal{L}\,d\tau + \sum_j g_s\left(\int_0^\beta \rho_j\,d\tau\right)\right], \tag{A20}$$

where the Lagrangian $\mathcal{L}(\rho, \psi^\pm)$ has the form

$$\begin{aligned}
\mathcal{L}(\rho,\psi^\pm) = \sum_{j,l}\Big[&\frac{1}{2}\rho_j\mathcal{J}_{jl}^{-1}\rho_l - \psi_j^+\mathcal{J}_{jl}^{-1}\dot{\psi}_l^-\\
&+ \rho_j\mathcal{J}_{jl}^{-1}(\psi_j^-\psi_l^+ - \psi_l^-\psi_l^+)\\
&+ \frac{1}{2}\psi_j^-\psi_j^+\mathcal{J}_{jl}^{-1}\psi_l^-\psi_l^+\\
&- \frac{1}{2}\psi_j^-\mathcal{J}_{jl}^{-1}(\psi_l^-)^2\psi_l^+\Big],
\end{aligned} \tag{A21}$$

with $\mathcal{J}^{-1}$ being the inverse Jacobian (A16), and the function $g_s(x)$ is

$$\begin{aligned}
g_s(x) &= \mathcal{Q}_S(x) + \ln\left[\sinh\left(\int_0^\beta \frac{1}{2}\rho\,d\tau\right)\right]\\
&= \ln\left[\exp\left(\left(S+\frac{1}{2}\right)x\right) - \exp\left(-\left(S+\frac{1}{2}\right)x\right)\right],
\end{aligned} \tag{A22a}$$

$$\frac{d}{dx}g_s(x) = \frac{1}{2} + b_S(x) + n_0(x), \qquad n_0(x) = \frac{1}{e^x-1}. \tag{A22b}$$

4. One-loop equation for spontaneous magnetization

a. Integration measure in the perturbation approach

To prepare the integration measure over fields ρ_j, $\psi_j^\pm$ at the site $\boldsymbol{r}_j$, we note that in our system with a nonzero mean spin $\overline{S}_z$, the field $\rho_j(t)$ also has a nonzero mean value $\overline{\rho}$:

$$\rho(\boldsymbol{r}_j, t) \equiv \rho_j(t) = \overline{\rho} + \eta_j(t), \tag{A23}$$

where fluctuations $\eta_j(\boldsymbol{r}_j, t) \equiv \eta_j(t)$ are assumed to be small in some sense.

In our case of spatial and time homogeneity, it is customary to use Fourier components,

$$\psi_j^{\pm}(t) = \frac{1}{N_{\text{lat}}} \sum_{n,\boldsymbol{k}} \psi_{n,\boldsymbol{k}}^{\pm} \exp[\pm i(\omega_n \tau + \boldsymbol{k}\cdot\boldsymbol{r}_j)], \tag{A24a}$$

$$\eta_j(t) = \frac{1}{N_{\text{lat}}} \sum_{n,\boldsymbol{k}} \eta_{n,\boldsymbol{k}} \exp[i(\omega_n \tau + \boldsymbol{k}\cdot\boldsymbol{r}_j)]. \tag{A24b}$$

The equation for spontaneous magnetization follows from the identity

$$\langle \eta_j(\tau) \rangle = 0 \tag{A25}$$

valid for any j and τ due to the homogeneity. To compute this expectation value explicitly, we substitute the decomposition (A24) into (A20)–(A22a) and arrive at the measure of perturbative averaging over fluctuations around the mean field:

$$\mathcal{D}\eta\mathcal{D}\psi^{\pm} \exp(-\Gamma), \quad \text{where} \tag{A26a}$$

$$\Gamma = \Gamma^{(2)} + \Gamma^{(3)} + \Gamma^{(4)} - W\{\eta\}, \tag{A26b}$$

$$\Gamma^{(2)} = \sum_{n,\boldsymbol{k}} \frac{1}{J_{\boldsymbol{k}}} \left\{ \frac{|\eta_{n,\boldsymbol{k}}|^2}{2} [1 - \beta^2 J_{\boldsymbol{k}} g_s''(\beta\overline{\rho})\Delta(n)] + \psi_{n,\boldsymbol{k}}^{+}\psi_{n,\boldsymbol{k}}^{-} \left[i\omega_n + \overline{\rho}\left(1 - \frac{J_{\boldsymbol{k}}}{J_0}\right)\right]\right\}. \tag{A26c}$$

Hereafter, $\Delta(n)$ is the Kronecker delta defined as $\Delta(0) = 1$, and $\Delta(n \neq 0) = 0$. Furthermore,

$$\Gamma^{(3)} = \frac{1}{\sqrt{N}_{\text{lat}}} \sum_{n_{1,2,3},\boldsymbol{k}_{1,2,3}} \eta_{\boldsymbol{k}_1,n_1} \psi_{\boldsymbol{k}_2,n_2}^{+} \psi_{\boldsymbol{k}_3,n_3}^{-} \times Q_{\boldsymbol{k}_1,\boldsymbol{k}_2} \Delta(n_1 + n_2 - n_3)\Delta(\boldsymbol{k}_1 + \boldsymbol{k}_2 - \boldsymbol{k}_3), \tag{A26d}$$

$$Q_{\boldsymbol{k}_1,\boldsymbol{k}_2} = \frac{1}{J_{\boldsymbol{k}_2}} - \frac{1}{J_{\boldsymbol{k}_1}}, \tag{A26e}$$

$$\Gamma^{(4)} = \frac{1}{\sqrt{N}_{\text{lat}}} \sum_{n_{1,2,3,4},\boldsymbol{k}_{1,2,3,4}} T_{\boldsymbol{k}_{1,2};\boldsymbol{k}_{3,4}} \psi_{\boldsymbol{k}_1,n_1}^{+} \psi_{\boldsymbol{k}_2,n_2}^{+} \psi_{\boldsymbol{k}_3,n_3}^{-} \psi_{\boldsymbol{k}_4,n_4}^{-} \times \Delta(n_1 + n_2 - n_3 - n_4)\Delta(\boldsymbol{k}_1 + \boldsymbol{k}_2 - \boldsymbol{k}_3 - \boldsymbol{k}_4), \tag{A26f}$$

$$T_{\boldsymbol{k}_{1,2};\boldsymbol{k}_{3,4}} = \frac{1}{4}\left(\frac{1}{J_{\boldsymbol{k}_1-\boldsymbol{k}_2}} + \frac{1}{J_{\boldsymbol{k}_2-\boldsymbol{k}_4}} - \frac{1}{J_{\boldsymbol{k}_1}} + -\frac{1}{J_{\boldsymbol{k}_2}}\right). \tag{A26g}$$

Vertex $T_{\boldsymbol{k}_{1,2};\boldsymbol{k}_{3,4}}$ is independent of Matsubara frequencies ω_n, and, due to the conservation law of momentum, it is symmetric with respect to the permutation $\boldsymbol{k}_3 \leftrightarrow \boldsymbol{k}_4$.

Last but not least, the contribution to Γ in (A26b), denoted as $W\{\eta\}$, is an infinite series over fluctuations $\eta_{\boldsymbol{k}} \equiv \eta_{n=0,\boldsymbol{k}}$ with zero Matsubara frequencies:

$$W\{\eta\} = \sum_m N^{(1-m/2)} \frac{\beta^m}{m!} \sum_{\boldsymbol{k}_1,\ldots,\boldsymbol{k}_m} \Delta(\boldsymbol{k}_1 + \cdots + \boldsymbol{k}_m) \times g_s^{(m)}(\beta\overline{\rho})\eta_{\boldsymbol{k}_1}, \ldots, \eta_{\boldsymbol{k}_m}, \tag{A27a}$$

$$g_s^{(m)}(x) = \left(\frac{d}{dx}\right)^m g_s(x). \tag{A27b}$$

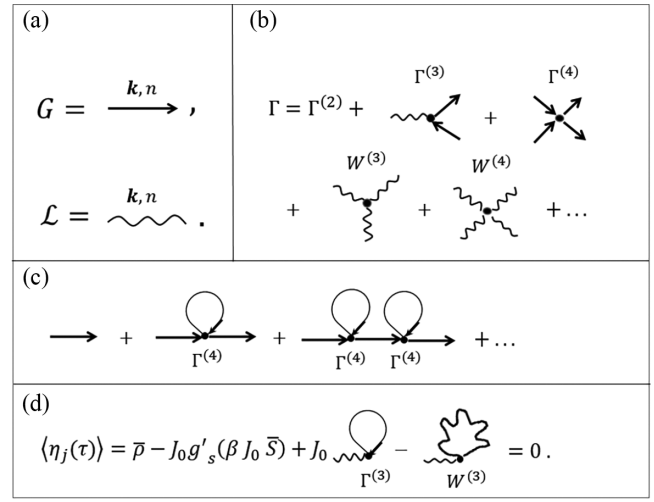

FIG. 4. (a) Graphical notation for the correlators $G_0(\omega_n, \boldsymbol{k})$ and $\mathcal{L}_0(\omega_n, \boldsymbol{k})$. (b) Notation for vertices $\Gamma^{(3)}$, $\Gamma^{(4)}$, $W^{(3)}$, and $W^{(4)}$. (c) One-loop renormalization of the frequency spectrum. (d) The one-loop equation for magnetization.

b. Magnetization in the first order in $1/Z$

Seed correlation functions are diagonal in $\boldsymbol{k}$ and ω_n:

$$G_0(\omega_n, \boldsymbol{k}) = \langle \psi_{n,\boldsymbol{k}}^{+} \psi_{n,\boldsymbol{k}}^{+} \rangle = J_{\boldsymbol{k}} \left[i\omega_n + \frac{(J_0 - J_{\boldsymbol{k}})\overline{\rho}}{J_0} \right]^{-1},$$

$$\mathcal{L}_0(\omega_n, \boldsymbol{k}) = \langle \eta_{n,\boldsymbol{k}} \eta_{-n,-\boldsymbol{k}} \rangle = \frac{J_{\boldsymbol{k}}}{1 - \beta^2 J_{\boldsymbol{k}} g_S''(\beta\overline{\rho})\Delta(n)}. \tag{A28}$$

Graphical notations for correlators $G_0(\omega_n, \boldsymbol{k})$ and $\mathcal{L}_0(\omega_n, \boldsymbol{k})$ are shown in Fig. 4 together with graphical notations for vertexes $\Gamma^{(3)}$, $\Gamma^{(4)}$, and W, defined by Eqs. (A26d), (A26f), and (A27).

The one-loop renormalization of the Green function G depicted in Fig. 4(c) is equivalent to substituting $\bar{\rho} \to J_0\bar{S}$ in the expression (A28) for G_0. Additionally, the regularization of simultaneous field products related to the initial spin problem follows the Stratonovich rule [36] rather than relying on chronological ordering. It is equivalent to a symmetrical $n \to -n$ cutoff in summation over Matsubara frequencies. It gives

$$\langle \psi_{\boldsymbol{k}}^{-} \psi_{\boldsymbol{k}}^{+} \rangle = J_{\boldsymbol{k}} \left(\frac{1}{2} + n_{\boldsymbol{k}} \right), \quad n_{\boldsymbol{k}} = \frac{1}{e^{\beta E_{\boldsymbol{k}}} - 1}. \tag{A29}$$

It can be verified that Eq. (A29), along with Jacobian (A16), is consistent with the kinematic identities (22) described in Sec. III B. For example, in the case in which $J_{nn'} \propto \delta_{nn'}$, the free energy is proportional to $S(S+1)$.

Note that Eq. (A25) for $\langle \eta \rangle$ represents the sum of connected diagrams. In the one-loop approximation, we have the terms shown in Fig. 4(d). By substituting the analytical expressions for the propagators and vertices provided above, we arrive at Eq. (12).

[1] T. Mairoser, A. Schmehl, A. Melville, T. Heeg, L. Canella, P. Böni, W. Zander, J. Schubert, D. E. Shai, E. J. Monkman, K. M. Shen, D. G. Schlom, and J. Mannhart, Is there an intrinsic limit to the charge-carrier-induced increase of the Curie temperature of EuO? Phys. Rev. Lett. **105**, 257206 (2010).

[2] B. T. Matthias, R. M. Bozorth, and J. H. Van Vleck, Ferromagnetic interaction in EuO, Phys. Rev. Lett. **7**, 160 (1961).

[3] K. Ahn and J. Suits, Preparation and properties of EuO films, IEEE Trans. Magn. **3**, 453 (1967).

[4] M. Shafer, J. Torrance, and T. Penney, Relationship of crystal growth parameters to the stoichiometry of EuO as determined by I.R. and conductivity measurements, J. Phys. Chem. Solids **33**, 2251 (1972).

[5] S. Burg, V. Stukalov, and E. Kogan, On the theory of indirect exchange in EuO, Phys. Status Solidi B **249**, 847 (2012).

[6] P. Sinjukow and W. Nolting, Metal-insulator transition in EuO, Phys. Rev. B **68**, 125107 (2003).

[7] Y. Shapira, S. Foner, and T. B. Reed, Euo. I. Resistivity and Hall effect in fields up to 150 kOe, Phys. Rev. B **8**, 2299 (1973).

[8] V. Cherepanov, I. Kolokolov, and V. L'vov, The Saga of YIG: Spectra, thermodynamics, interaction and relaxation of magnons in a complex magnet, Phys. Rep. **229**, 81 (1993).

[9] L. Passell, O. W. Dietrich, and J. Als-Nielsen, Neutron scattering from the Heisenberg ferromagnets EuO and EuS. I. The exchange interactions, Phys. Rev. B **14**, 4897 (1976).

[10] J. Als-Nielsen, O. W. Dietrich, and L. Passell, Neutron scattering from the Heisenberg ferromagnets EuO and EuS. II. Static critical properties, Phys. Rev. B **14**, 4908 (1976).

[11] H. Mook, Temperature dependence of the spin dynamics of EuO, Phys. Rev. Lett. **46**, 508 (1981).

[12] J. C. Le Guillou and J. Zinn-Justin, Critical exponents for the n-vector model in three dimensions from field theory, Phys. Rev. Lett. **39**, 95 (1977).

[13] A. S. Borukhovich, M. S. Marunya, V. G. Bamburov, N. I. Ignat'eva, and P. V. Gel'd, Critical phenomena in EuO, Zh. Eksp. Teor. Fiz. **69**, 565 (1976) [Sov. Phys. JETP **42**, 288 (1976)].

[14] P. Liu, J. A. Colon Santana, Q. Dai, X. Wang, P. A. Dowben, and J. Tang, Sign of the superexchange coupling between next-nearest neighbors in EuO, Phys. Rev. B **86**, 224408 (2012).

[15] P. Weiss, L'hypothèse du champ moléculaire et la propriété ferromagnétique (The molecular field hypothesis and the ferromagnetic property), J. Phys. Theor. Appl. **6**, 661 (1945).

[16] W. Heisenberg, On the theory of ferromagnetism, Z. Phys. **49**, 619 (1928).

[17] V. G. Bar'yakhtar, V. N. Krivoruchko, and D. A. Yablonski, Spin green functions and the problem of summation over physical states, Sov. Phys. JETP **58**, 351 (1983).

[18] V. G. Vaks, A. I. Larkin, and S. A. Pikin, Thermodynamics of an ideal ferromagnetic substance, Zh. Eksp. Teor. Fiz. **53**, 281 (1967) [Sov. Phys. JETP **26**, 188 (1968)].

[19] V. G. Vaks, A. I. Larkin, and S. A. Pikin, Spin waves and correlation functions in a ferromagnetic, Zh. Eksp. Teor. Fiz. (U.S.S.R.) **53**, 1089 (1967) [Sov. Phys. JETP **26**, 647 (1968)].

[20] V. I. Belinicher and V. S. L'vov, Spin diagram technique for nonequilibrium processes in the theory of magnetism, Zh. Eksp. Teor. Fiz. **86**, 967 (1984) [Sov. Phys. JETP **59**, 584 (1984)].

[21] L. Landau and E. Lifshitz, *Statistical Physics* (Pergamon Press, Oxford, 1970), Vol. 5.

[22] M. Mohseni, V. I. Vasyuchka, V. S. L'vov, A. A. Serga, and B. Hillebrands, Classical analog of qubit logic based on a magnon Bose–Einstein condensate, Commun. Phys. **5**, 196 (2022).

[23] J. Van Vleck, A survey of the theory of ferromagnetism, Rev. Mod. Phys. **17**, 27 (1945).

[24] W. Heisenberg, Mehrkörperproblem und resonanz in der Quantenmechanik, Z. Phys. **38**, 411 (1926).

[25] M. Chertkov and I. Kolokolov, Equilibrium and nonequilibrium mean-field dynamics of quantum spin claster, Zh. Eksp. Teor. Fiz. **106**, 1525 (1994) [JETP **79**, 824 (1994)].

[26] M. Chertkov and I. Kolokolov, Equilibrium dynamics of a paramagnetic cluster, Phys. Rev. B **51**, 3974 (1995).

[27] R. V. Chamberlin, Mean-field cluster model for the critical behavior of ferromagnets, Nature (London) **408**, 337 (2000).

[28] S. Tyablikov, *Methods in the Quantum Theory of Magnetism* (Springer, Dordrecht, 1967).

[29] E. Praveczki, Fiz. Met. Metalloved (USSR) **12**, 296 (1961).

[30] H. B. Callen, Green function theory of ferromagnetism, Phys. Rev. **130**, 890 (1963).

[31] E. Praveczki, Free spin-wave theory renormalised in respect of temperature, Phys. Lett. **6**, 147 (1963).

[32] Y. A. Izyumov and Y. N. Skryabin, *Statistical Mechanics of Magnetically Ordered Systems* (Springer, Dordrecht, 1988).

[33] I. Kolokolov, Functional representation for the partition function of the quantum Heidenberg ferromagnet, Phys. Lett. A **114**, 99 (1986).

[34] I. Kolokolov and E. Podivilov, Functional method for quantum ferromagnets and non-Magnon dynamics at low temperatures, Sov. Phys. JETP **68**, 119 (1989).

[35] J. Hubbard, Calculation of partition functions, Phys. Rev. Lett. **3**, 77 (1959).

[36] R. Stratonovich, On a method of calculating quantum distribution functions, Sov. Phys. Dokl. **2** (1958).